

Improved EMC of Switched-Mode Power Converters with Randomized Modulation

DOI 10.7305/automatika.53-2.166
UDK 621.314.5.013/6.013:621.317
IFAC 3.1

Original scientific paper

This paper surveys some analytical and experimental results concerning different randomized modulation strategies in switched-mode power converters (SMPCs). After a short review of practical experiences within the literature it presents the benefits of several randomized schemes for power converters (i.e. reduced electromagnetic interference - EMI, and lower acoustic noise). It also introduces the mathematical background for dealing with randomized modulation within the medium-frequency range: power spectrum density (PSD). Finally, the EMI measurements confirm the improved EMC performances of the randomized boost rectifier, as also in the DC-DC buck converter.

Key words: Switched-mode power converters (SMPCs), Randomized pulsewidth modulation (RPWM), Electromagnetic compatibility (EMC), Power spectral density (PSD)

Poboljšana elektromagnetska kompatibilnost (EMC) sklopnog energetskeg pretvarača sa slučajnom modulacijom. Ovaj članak istražuje analitičke i eksperimentalne rezultate različitih slučajnih strategija modulacije u sklopnim energetskim pretvaračima (SMPCs). Nakon kratkog pregleda praktičnih iskustava iz literature, predstavljene su prednosti nekoliko slučajnih shema za energetske pretvarače (smanjena elektromagnetska interferencija - EMI, i niži akustični šum). Također, uvedena je matematička podloga za rad sa slučajnom modulacijom u području srednjih frekvencija: spektralna gustoća snage (PSD). Konačno, EMI mjerenja potvrđuju poboljšanja EMC performansi slučajnih uzlaznih ispravljača, kao i DC-DC silaznih pretvarača.

Ključne riječi: sklopni energetski pretvarači (SMPCs), slučajna širinsko-impulsna modulacija (RPWM), elektromagnetska kompatibilnost (EMC), spektralna gustoća snage (PSD)

1 INTRODUCTION

Recently, the electromagnetic compatibility (EMC) regulations for fast switching power electronic converters (SMPCs) have become tighter than ever [1]. The conversion of electrical power is carried-out using fast semiconductor switching devices, which are utilized within various modern equipment where reducing losses is the designer's main concern [2]. A fast switching operation generates signals with high voltage-rate (du/dt) and high current rate (di/dt) and, consequently, disturbances over wider frequency bandwidths [3]. These voltage and current slew-rates and spikes induce large AC displacement currents in both physical and parasitic circuit elements. The displacement currents can create excessive noise in two forms: conducted noise (in connecting wires, busses, and ground planes) as conducted to an other circuitry and, radiated noise (capacitively-coupled current to the element's case or heat-sink) which is transformed to voltage and then radiated to other circuitry. Such noises can never be fully eliminated, however, they can only be attenuated to those

levels conforming to accepted regulatory limits [4, 5].

Conductive noise has two major sources: the first one results from the distorted input current of a converter [6] and, from the reflected ripple-current at its input into the converter [4]. The second one is due to the noise of voltage-switching at the main power switch. Although switching converters produce significant amounts of switching noise, they are also required to operate in EMC sensitive applications. In this case, the device has to satisfy, not only the electrical requirements but also the EMI regulations, such as EN55022 for the information technology equipment [4] or EN55025 for the automotive environment [5]. Increasing the number of electrical motors in modern cars (water pump for windshield cleaning, wipers, mirrors, seats etc.) require the need for switched-mode power converters (SMPCs) when driving these motors. The influence of the converter's reflected input current-ripple on the rest of the supplying current can be mostly reduced by integrating the numerous diversities of the EMI filters. Other advanced techniques for EMI reductions propose active gate-drivers. One

active gate-driver uses so-called flank-shaping techniques, where the power transistor gate-signal is shaped and/or controlled in such a way as to determine optimal transistor drain di/dt or drain-source du/dt , resulting in an EMC-friendly SMPC operation. Different random modulation strategies are proposed in [7] for improving power spectral density (PSD) and conductive EMI reduction, but without experimental proof. A chaotically modulated OFF-time current mode control for DC-DC boost converter which also spreads the inductor current spectrum is presented in [8].

This paper is organized as follows. The next section classifies different randomized switching and introduces basic mathematical concepts - the average autocorrelation and the power spectrum density. Section 3 presents the randomized PWM boost rectifier with improved wide-band EMC and, section 4 describes the benefits of randomized modulation against the normal PWM within the synchronous DC-DC converter structure from PSD analysis to the EMI measurements. Section 5 concludes this paper.

2 RANDOMIZED SWITCHING SIGNAL ANALYSIS: POWER SPECTRAL DENSITY

Over the last four decades, SMPCs designers have implemented randomized switching for different reasons. Initially, the randomized switching concept was introduced within the self-commutated thyristor DC-DC converter for reducing acoustical noise because of low-frequency switching [9]. Faster semiconductor switching devices eventually offered a simple solution to the acoustic noise problem (at least during DC-DC conversion) and, randomized switching was set aside.

Fourier methods are commonly used for signal analysis and system design [10]. In this case, this method is used mostly for SMPC voltage and current analysis. By sampling the signals using a digital oscilloscope (with the maximum number of samples N), Discrete Fourier transform (DFT) can be calculated off-line by using Matlab [11]. In order to obtain DFT, the continuous frequency domain of discrete time Fourier transform (DTFT) is sampled at N points, uniformly spaced around the unit circle within the z -plane, i.e., at points $\omega_k = (2\pi k/N)$, $k = 0, 1, \dots, N - 1$, as shown in (1). The signal $s[n]$ is either a finite-length sequence of length N , or it is a periodic sequence with period N :

$$S[k] = \sum_{n=0}^{N-1} s[n] e^{-j2\pi kn/N}, \quad k = 0, 1, \dots, N - 1 \quad (1)$$

2.1 Characteristics of Random Modulation Schemes

From several randomized modulation strategies, four of them are more favorable (see Table 1): random pulse-position modulation (RPPM), random pulse width modulation (RPWM), and random carrier-frequency modulation

Table 1. Characteristics of different random switching schemes

Modulation	T_{Sk}	α_k	ε_k	$d_k = \alpha_k/T_{Sk}$
PWM	const.	const.	0	const.
RPPM	const.	const.	rand.	const.
RPWM	const.	rand.	0	rand.
RCFMFD	rand.	rand.	0	const.
RCFMVD	rand.	const.	0	rand.

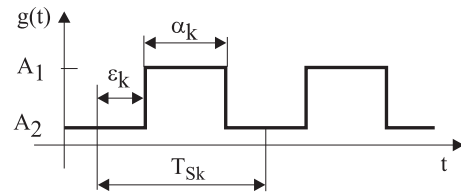


Fig. 1. Switching signal in randomized modulation scheme

with a fixed duty cycle (RCFMFD), or with a variable duty cycle (RCFMVD), as considered in [7]. However, any effectiveness of EMI reduction in each random modulation scheme, regarding DC-DC converters was experimentally unconfirmed, except in [3].

The characteristics of the switching pulse in each modulation scheme are summarized in Table 1, with the aid of Fig. 1. The switching function $g(t)$ has two discrete levels (namely A_1 and A_2), which are applicable for describing the behavior of classical DC-DC converters. T_{Sk} is the duration of the k -th cycle. α_k is the duration of the gate pulse in the k -th cycle and ε_k is the delay time of the gate pulse. The duty cycle of the switch d_k in the k -th cycle is equal to α_k/T_{Sk} .

RPPM is similar to the classical PWM scheme with constant switching frequency. However, the position of the gate pulse is randomized within each switching period, instead of commencing at the start of each cycle. RPWM allows the pulse width to vary but the average pulse width is equal to the required duty cycle. RCFMFD exhibits a randomized switching period and constant duty cycle, whilst RCFMVD exhibits a randomized switching period and constant pulse width. As the pulse width in RCFMVD is fixed and the switching period is randomized, the resultant duty cycle is also randomized. Nevertheless, the average duty cycle is equal to the desired value.

2.2 The Level of Randomness

In order to investigate the effectiveness of the stochastic variable randomness level on spreading harmonic power, a randomness level \mathfrak{R} for each scheme is defined. For RPPM,

$$\mathfrak{R}_{RPPM} = \frac{\varepsilon_2 - \varepsilon_1}{T_S}, \quad (2)$$

where $\varepsilon_k \in [\varepsilon_1, \varepsilon_2]$. ε_1 and ε_2 are the minimum and maximum limits of the pulse positions within each cycle. ε_1 is obviously equal to zero. T_S is the nominal switching period.

For RPWM,

$$\mathfrak{R}_{RPWM} = \frac{\alpha_2 - \alpha_1}{T_S} = d_2 - d_1, \quad (3)$$

where $\alpha_k \in [\alpha_1, \alpha_2]$. Thus, the duty cycle d_k varies between the minimum possible value d_1 and the maximum possible value d_2 around the nominal duty cycle within the classical PWM scheme.

For RCFMFD and RCFMVD:

$$\mathfrak{R}_{RCFMFD} = \mathfrak{R}_{RCFMVD} = \frac{T_2 - T_1}{T_S} \quad (4)$$

In these two modulation schemes, T_{Sk} varies between a minimum possible value T_1 and a maximum possible value T_2 . The duty cycle d_k in RCFMVD varies between $[(\alpha_k/T_2), (\alpha_k/T_1)]$, in which α_k is fixed.

2.3 Power Spectral Density – PSD

In the case of the randomized modulation scheme the harmonic spectrum is random and different each time, therefore, it must be evaluated by an appropriate mathematical tool. When considering the random process theory, the obvious quantity to study within a randomized switching setup is the power spectrum (the Fourier transform – FT of the autocorrelation function of a signal), and not the harmonic spectrum (i.e. the FT of the signal itself) [12–14]. In particular, the autocorrelation function of a random process is the appropriate statistical average concerning the characterizations of random signals within the time-domain. The FT of the autocorrelation function gives the PSD and provides transformation from the time-domain to the frequency-domain.

Let $X_{2W}(f)$ denote the FT of the symmetrically truncated version of time signal $x(t)$ with double width (i.e. input current or voltage of SMPC), extending from $-W$ to $+W$. An important result of the Fourier theory shows that if signal $x(t)$ is a wide-sense stationary process, then PSD is related to $X_{2W}(f)$ as follows [15]:

$$\text{PSD} = \lim_{W \rightarrow \infty} E \left\{ \frac{1}{2W} |X_{2W}(f)|^2 \right\}, \quad (5)$$

where the expectation operator $E[\cdot]$ takes over the whole ensemble and the quantity $(1/2W)|X_{2W}(f)|^2$ is called the periodogram of the random process $x(t)$. Usually, a 50 % overlap between the data segments contained in the appropriate window is proposed [15]. This produces good results

in many applications, but does not always improve the situation significantly [12]. The well known Welch's estimation method for PSD is also implemented within Matlab software package as the "psd" function:

$$\text{PSD} = \text{psd}(X, \text{NFFT}, \text{Fs}, \text{Window}, \text{NOverlap}, \text{DTrend}).$$

According to the significant characteristics of each particular window - the best asymptotic sidelobe decay rate and a sufficient low sidelobe level as well - Hanning window was chosen and used in all estimations, and the results were experimentally verified within a high-power-factor boost rectifier and in the buck SMPC.

2.4 Electromagnetic Interference – EMI

The rapid changes in voltages and currents within the SMPCs are a source of EMI with other equipment, as well as with its own proper operation. The EMI is transmitted in two forms: *radiated* and *conducted* noises. Conducted noise (as shown in Fig. 2) consists of two categories commonly known as the *differential mode voltage* - U_{dm} (symmetrical) and the *common mode voltage* - U_{cm} (asymmetrical). The differential mode current i_{dm} is conducted at the connecting line from source to sink, and back. The common mode current i_{cm} is formed through the power lines, parasitic capacitance C_p and earth-ground line, back to the source of the interference. Both, differential mode and common mode noises are generally present on the input and the output lines. Any filter design has to take into account both of these noise modes.

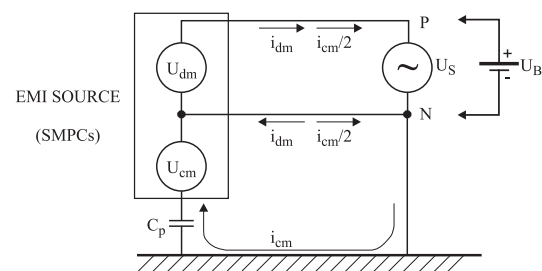


Fig. 2. Conducted interference mechanism in SMPCs

There are numerous EMC regulations present in practice, to provide the user with safe and quality products that are in compliance with certain EMI requirements. The more effective EMI regulatory bodies are CISPR, IEC, VDE, EN and FCC for specifying the maximum limit for the allowed EMI. In order to compare equipments against these limits, the conducted noise was measured by means of a specified Line Impedance Stabilization Network - LISN, and by using the industrial (or precompliance) EMI receiver Rohde & Schwarz ESHS10 (or ESPI 100371). In

order to fulfill standard EN55022 (or EN55025), the conducted electrical noise measurement had to be made by a quasi-peak voltage detector within a frequency range from 150 kHz to 30 MHz (or 108 MHz).

3 SMPC 1: BOOST RECTIFIER (HPFCC)

A single-phase diode bridge rectifier has a very strong and undesirable influence on the main. Traditionally, in this case, bulky passive filters have been used to clean harmonics from the main [16]. Another solution for improving the harmonic spectrum of the input current is offered by using a high power factor correction circuit (HPFCC) with a boost converter [17]. The stability problem of three-phase PWM rectifier with LCL filter, is analyzed in [18].

The conventional scheme of the HPFCC with control set-up is shown in Fig. 3. The necessary feedback control signals are combined with these reference values to specify the modulating signal $m(t)$, which in turn determines duty ratio $d(t)$. Since a power converter generally operates within a periodic steady state with a chosen switching frequency, the influence of the pulse width modulation (PWM) can be directly detected in the harmonic content of the waveform. By power factor correction through a high-frequency switching current control mode, another problem arises: high-frequency harmonics are generated by the converter in radio-frequency (RF) range. Therefore, the EMI problem produced due to high-rates of di/dt and du/dt must also be considered in HPFCC.

For this reason, randomization can change the harmonic content of the input current without excessively affecting the proper operation of the boost rectifier and may avoid the need for redesigning the system. Randomized changing of period T_S in the ramp generator results in randomly 'dithering' the duty ratio $d(t)$ from its nominal operational

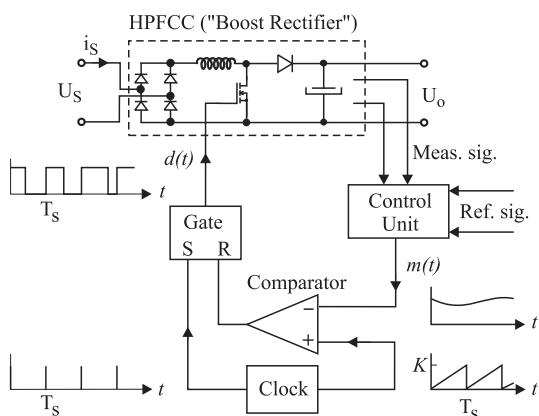


Fig. 3. High power factor correction circuit and control set-up

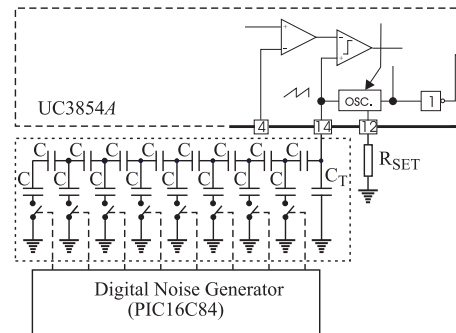


Fig. 4. Capacitive network and digital random-noise generator

point. There are many commercial control units available on the market and in our case the Unitrode chip UC-3854A (suitable for current control mode) was used. The central switching frequency of the ramp generator in the control-unit is defined by an appropriate setting of time constant with chosen C_T and R_{SET} (Fig. 4). If capacitance C_T is varied by using an particular network of additional capacitors, which are then switched by a digital random-noise generator, the slope of the PWM ramp generator in the control-unit also changes randomly. The white-noise generator is realized by using the microcontroller PIC-16C84. This microcontroller randomly generates 8-bit switching states at the output to switch ON and OFF an appropriate capacitor on the ladder, which then dithers the carrier frequency in a randomized manner within the region:

$$\frac{1.25}{C_T R_{SET}} < f_S < \frac{1.25}{(C_T + 0.618C) R_{SET}} \quad (6)$$

3.1 Wide-band Frequency Analysis of the HPFCC

The time to address Electromagnetic Compatibility (EMC) is before it becomes an expanding problem [1]. Proper attention to EMC from the design-stage through to pre-certification testing can reduce product-development time and cost. Traditional EMC measuring equipment is very costly, therefore experimental frequency-analysis over the wide range is proposed requiring minimum measurement instruments: a digital storage oscilloscope and a personal computer running Matlab.

Firstly, the low-frequency harmonic content of the boost rectifier is considered. Since the RPWM principle is introduced into an ordinary PWM control unit of the boost rectifier in order to achieve a spread spectrum, this results in a small increase in the THD of the line current (from 5.31 % to 6.04 %), and a negligible decrease in the PF (from 0.9986 to 0.9982) as shown in Fig. 5. Compliance with the IEC 1000-3-2 Class A harmonics limit is verified by dashed-line. In order to eliminate the influences of all

other equipment connected to the main during the experiment, an extra sine-wave laboratory generator was used. It could be realized, that all the harmonics were well-below the limitations.

As realized in Section 2.3, best PSD estimations were made by using the Hanning window with the depicted parameters from several estimations, and the results were experimentally verified in (Fig. 6). Investigations confirmed that using the appropriate window length is much more critical for PSD estimation than using weak- or strong-overlapping. It was also evident that all the power of the switching frequency in the case of PWM switching control was dissipated up to the second PWM carrier harmonic, whilst in the case of the RPWM switching-control the PSD was dispersed. This result offers a good prediction method for reducing conducted EMI by using RPWM switching-control in a boost rectifier.

Finally, to compare against the EN55022 limits, the conducted noise was measured by using of specified LISN, consisting of $(5\Omega + 50\mu H) \parallel 50\Omega$, and by using the industrial EMI receiver Rohde & Schwarz ESHS10. In order to meet the EMI regulations, the measures of the conducted electrical noise were done by a quasi-peak voltage detector within a frequency-range from 160 kHz to 30 MHz. In the output protocol of Fig. 7 there were two limits present in order to quantify the measures: the first one (QP-limit) corresponding to the quasi-peak limit and the second (AVG-limit) corresponding to the average limit. Several measurements, modifications and improvements within the circuit were necessary in order to comply with the EMI standard limitations (see Fig. 7). Conducted noise was measured in the cases of PWM control (solid-line) and RPWM control (dashed-line). It is evident, that the implementation of RPWM control had reduced the conducted EMI to a sufficient quantity, as already expected from the power spec-

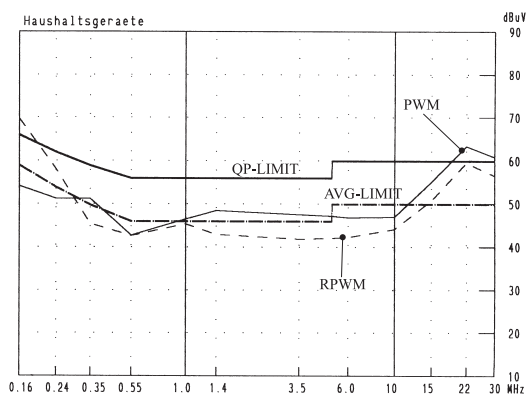


Fig. 7. Final measures of the conducted EMI with PWM- (solid-line), and the RPWM switching-control (dashed-line)

trum in Fig. 6(a) and (b), respectively. A smaller increment of conducted noise at the beginning of the frequency range, in the case of RPWM control was produced by the introduction of a noise signal to the switching function within the control unit.

4 SMPC 2: BUCK CONVERTER VS. HALF-BRIDGE INVERTER

Different chopper drives are used, in practice, for controlling the armature voltage of a DC motor and circuit arrangement, as shown in Fig. 8(a). Nowadays, the copper switch is usually a fast power MOSFET with very short switching times and low $R_{DS(on)}$ resistance, which reduces conductive losses but also produces extremely high voltage-rates (and current-rates) and therefore high EMI. It can be deduced from Fig. 8(a), that the minimal output voltage of the buck converter is always equal to the diode voltage drop $U_D \approx -0.6$ V. In order to achieve higher conversion efficiency, the synchronous rectifier configuration (i.e. half-bridge inverter) was investigated, where the conductive losses of the output MOSFET M_2 were lower than in the first case of the buck converter.

The hardware in Fig. 8(a) consists of an 8-bit PIC16F876 μ -controller, a programmable GAL16V8 logical device (PLD), and a half-bridge leg of two IRL2505 MOSFET power switches with IR2125 gate drivers. For

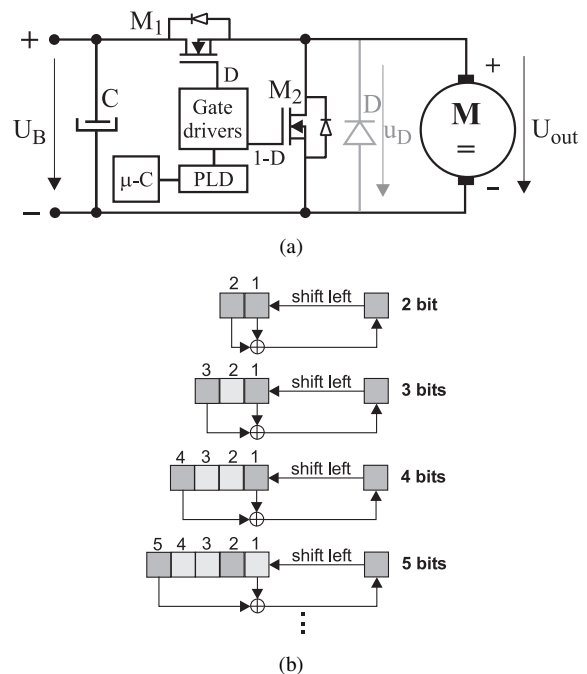


Fig. 8. DC motor drives alternative: (a) buck converter or synchronous rectifier (half-bridge inverter), (b) digital random generator - principle of operation

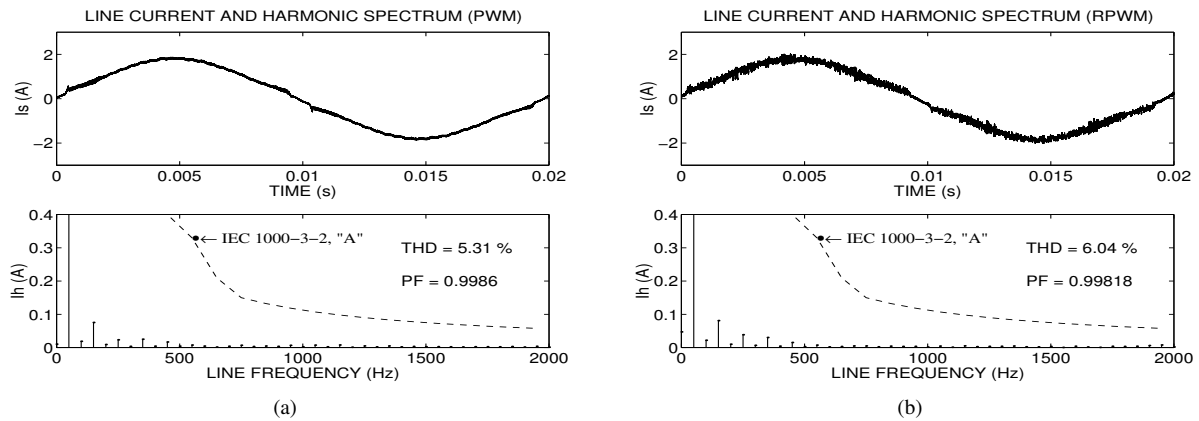


Fig. 5. Low-order harmonic analysis of the input current

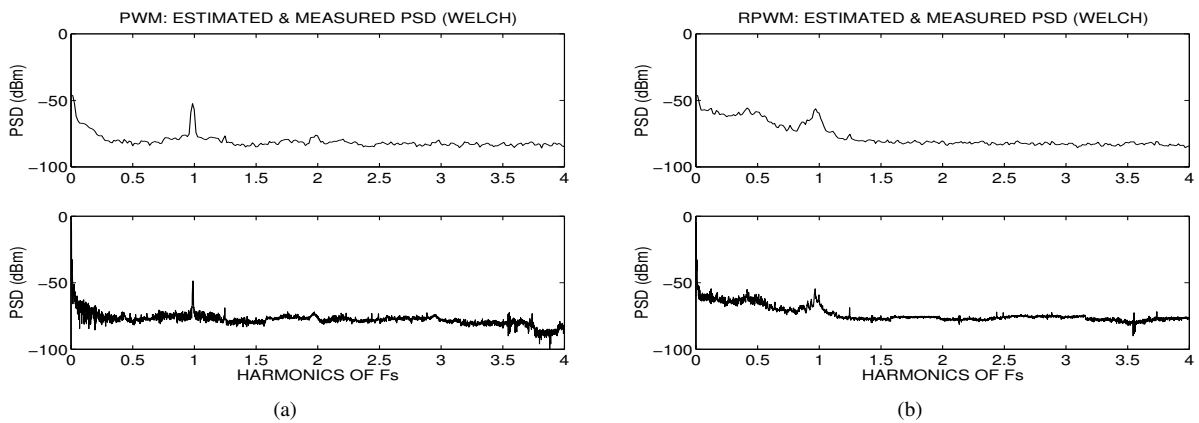


Fig. 6. Estimated (upper-traces) and measured PSD (lower-traces) of the input current in the boost rectifier

20 kHz PWM signal generation, 20 MHz CPU clock was used with a 250 timer-period value. For the RPWM generation, the same principle was used with periodic interruptions for changing RPWM duty cycle, as shown in Fig. 8(b). As random number generator Watson algorithm was used where the main operations were only XOR and shifting thus ensuring short execution time. When a random number within a certain bit resolution (4 bit resolution was mainly used for the basic operation and 5 bit resolution for extended randomization level). A similar solution can be found in the hybrid random PWM scheme of the motor drive, where pseudo-random binary sequences (PRBS) is used for acoustic noise reduction [19].

4.1 Wide-band Frequency Analysis of the HB Inverter

The average motor voltage in Fig. 8(a) is

$$U_{out} = DU_B, \quad (7)$$

where D is the duty ratio of the chopper. In a conventional DC-DC buck converter, the output voltage is generally sta-

bilized by the LC low-pass output filter and controlled by varying the duty cycle to the main switch. The duty cycle and switching frequency are kept constant within a steady-state operation, so that the harmonic power of the input-current and output-voltage are concentrated on the switching frequency multiples. Using the various random switching schemes presented in Table 1, the harmonic power within the frequency domain can be spread and the peak level of the PSD becomes less than that of the conventional PWM scheme. Discrete harmonics are significantly reduced and the harmonic power is also spread over a continuous noise spectrum of smaller magnitude, as reported in [12]. The spreading of the harmonic's energy across the spectrum may be carried out in various way. Several randomization schemes and their syntheses have been addressed in different papers, dealing with: random switching control in DC-DC converters [20], acoustic noise reduction in sinusoidal PWM inverters [21], or improving the EMC of the boost rectifier [3].

All PSD estimations for the DC-DC synchronous recti-

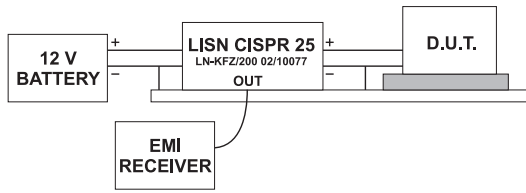


Fig. 10. Setup for CISPR 25 EMC measurement

fier’s (shown in Fig. 8(a)) output-voltage were carried out using Matlab software [11], and the results are shown in Fig. 9(a)-(d), respectively. The truth is, as many authors have reported, that spreading PSDs is a good prediction for reaching reduced conductive EMI at the input-terminals.

Active switching components such as semiconductor power transistors and diodes are the main noise sources in SMPCs, especially the parasitic ringing voltages and currents of all switches. However, not only an exact active component model is needed to predict accurate ringing frequency, amplitude, overshoot, and rising/falling transient, but an electrical equivalent circuit of the printed circuit board (PCB) layout is also necessary.

The output-voltage switching edges (on/off) were analyzed to discover any potential sources of additional EMI. Exact SPICE simulations were also performed with special attention to the DC-link capacitor’s modeling during optimizing the final SMPC circuit. CISPR 25 is a regulation for automotive applications, prescribing noise levels that can be produced by those switching devices assembled in vehicles and boats [5]. Although this standard considers both conductive and radiated EMI, this article focuses only on the conductive. The main component used for conductive one EMI measurements are based on the CISPR 25 standard (see actual set-up in Fig. 10): they are DC power supply (usually a 12 V battery), a Line Impedance Stabilization Network (LISN), precompliance EMI receiver Rohde&Schwarz ESPI 100371 and, any device under test (D.U.T.) with load.

CISPR 25 regulations for conductive EMI measurement in frequency range between 150 kHz and 108 MHz is divided into five EMC classes where, in each class, noise magnitude in dB μ V is prescribed for each frequency interval (see Table 2). These intervals are the danger areas for interfering with other devices installed in automobiles (radio, CD player, mobile phone, security systems etc.). Each measurement is limited to 9 kHz bandpass for frequencies between 150 kHz to 30 MHz and, limited to 120 kHz bandpass in the frequency range from 30 MHz to 108 MHz. The measurement duration in each frequency bandpass is 10 ms [5]. In this paper, one optimized hardware test setup of the SMPCs (i.e. HB inverter shown in Fig. 8(a)) was tested against the CISPR 25 Class 5 requirements.

Table 2. EN55025 (CISPR 25) EMI noise limitation

EMC Class	Magnitude (dB μ V)									
	0,15 MHz to 0,3 MHz		0,53 MHz to 2 MHz		5,9 MHz to 6,2 MHz		30 MHz to 54 MHz		68 MHz to 108 MHz	
	Peak	Average	Peak	Average	Peak	Average	Peak	Average	Peak	Average
1	113	100	95	82	77	64	77	64	61	48
2	103	90	87	74	71	58	71	58	55	42
3	93	80	79	66	65	52	65	52	49	36
4	83	70	71	58	59	46	59	46	43	30
5	73	60	63	50	53	40	53	40	37	24

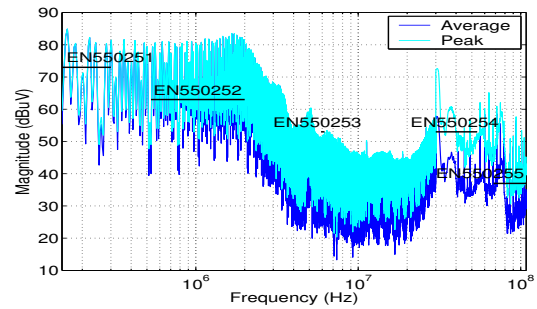


Fig. 11. Initial EMI measurement of the PWM SMPC

Regardless of the used switching topologies, awareness of commutation between power switches is recommended because it can distinguish conductive EMI sources. The initial measurement based on CISPR 25 standard for the buck converter from Fig. 8(a) is shown in Fig. 11. The switching frequency of the converter is 20 kHz with a average duty cycle of 70 %, and the power supply is 12 V. The load parameters are $R_L = 0.4 \Omega$, $L_L = 64 \mu\text{H}$ and with DC-link capacitors $4 \times 1000 \mu\text{F}$. It is evident that the EMI measurement in Fig. 11 shows a very non-compliant EMC result, where EMI noise magnitudes exceed the allowed conductive noise in each CISPR 25 Class 5 limit. The reason for this can be found in the non-optimized hardware set-up (bad driving circuit, PCB layout etc.) which also confirms oscillations in MOSFET’s output voltage at the turn-off sequence (shown in Fig. 12).

From the PSD estimation result in Fig. 9, all the proposed randomized modulation schemes in Table 1 were

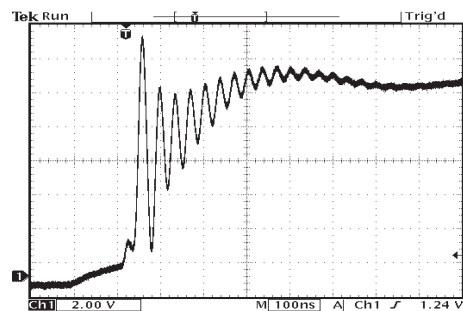


Fig. 12. Output voltage of the SMPC at the turn-off

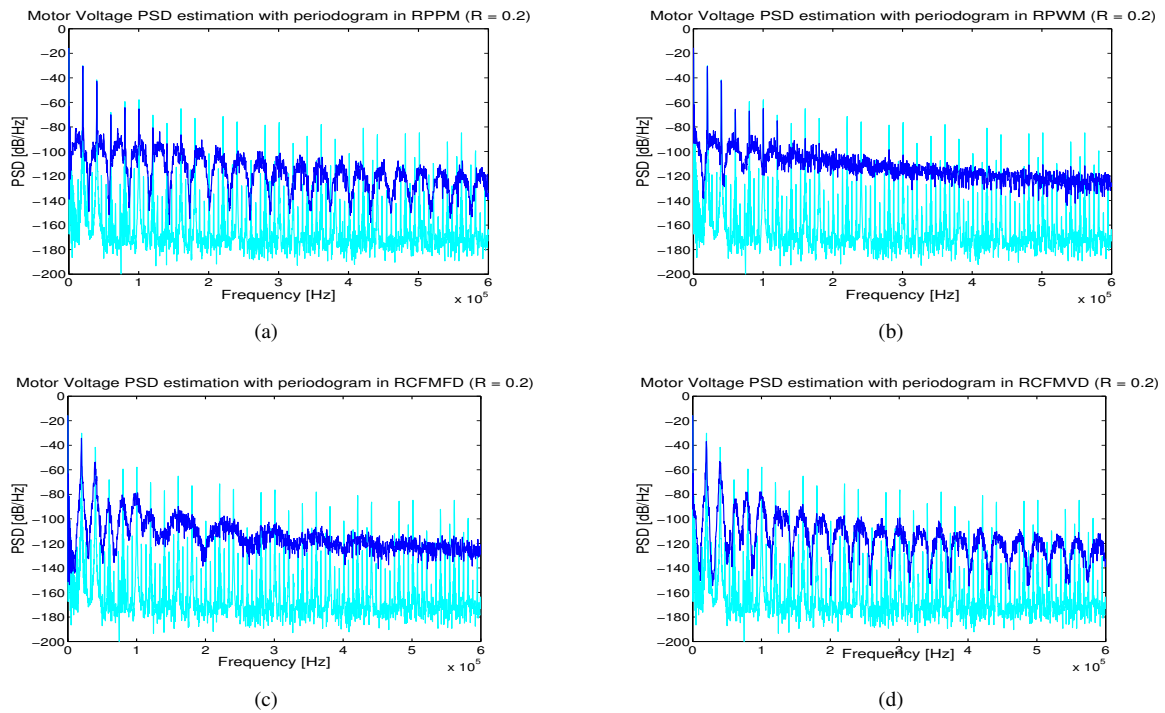


Fig. 9. PSD estimations of the output voltage at $\mathfrak{R} = 0.2$ against the PWM in DC-DC synchronous rectifier: (a) RPPM, (b) RPWM, (c) RCFMFD, (d) RCFMVD

performed on a buck converter by external driving, in order to reduce conductive EMI. Nevertheless, the randomness level was very high ($\mathfrak{R} = \pm 20\%$), and this was insufficient for reducing the conductive EMI noise below the CISPR 25 regulation (see Fig. 13 for the non-optimized SMPC board). In the case of RPPM in Fig. 13(a) the absolute values of the peak and average conductive noise was reduced over the whole frequency range with regard to the PWM result in Fig. 11. The result in the case of RPWM in Fig. 13(b) was even better, where the peak- and average-values of the conductive noise were smoothed, as in the case of RCFMFD (Fig. 13(c)). The last randomized modulation scheme RCFMVD in Fig. 13(d) was very similar to the RPPM result. Nevertheless, the limits of the CISPR 25 were exceeded in all considered randomized schemes, effective conductive noise reduction against PWM was evident within the range up to 2 MHz. In the range above 30 MHz unacceptable EMC could be found in the non-optimized driving circuit and high-speed digital signals transfer rate (du/dt). The source of the significant peak at the 30 MHz in all EMI measurements could be described as a switch commutation problem between the diode series inductance and junction capacitance. The oscillations at turn-off in Fig. 12 were eliminated and a smoother operation was also achieved (see Fig. 14).

Based on all measurements, the appropriate modulation

strategy for effective conductive noise reduction with minimal hardware configuration can be chosen in regard to low-price and high efficiency. An HB inverter (shown in Fig. 8(a)) driven by a PIC16F876 μ -controller with DCO as a processor clock, was rearranged. As can be seen in Fig. 13, the RCFMFD and RPWM modulation schemes were the more effective regarding conductive noise reduction, the second one being realized because of simpler hardware. The PIC's processor unit was numerically and peripherally insufficiently powerful for uploading all the described modulation schemes, therefore only the RPWM was implemented (as proposed in the block scheme of Fig. 8(b)).

It is important to note that the use of DCO led to higher EMI magnitudes at frequencies above 20 MHz therefore it was replaced by a quartz oscillator with a sinusoidal shape of output signal with distinct second and third harmonics (shown in Fig. 15). Using this modification in half-bridge SMPC with PWM modulation, the improved compatibility with CISPR 25 requirements is shown in Fig. 16. Single peak at 20 MHz was evident, but its higher harmonics did not harm the EMC of the SMPC any longer.

Since the set-up components and the topology of the SMPC had been optimized, the conductive EMI was evidently also reduced in the case of randomized PWM (see Fig. 17). The randomized PWM effectively reduced con-

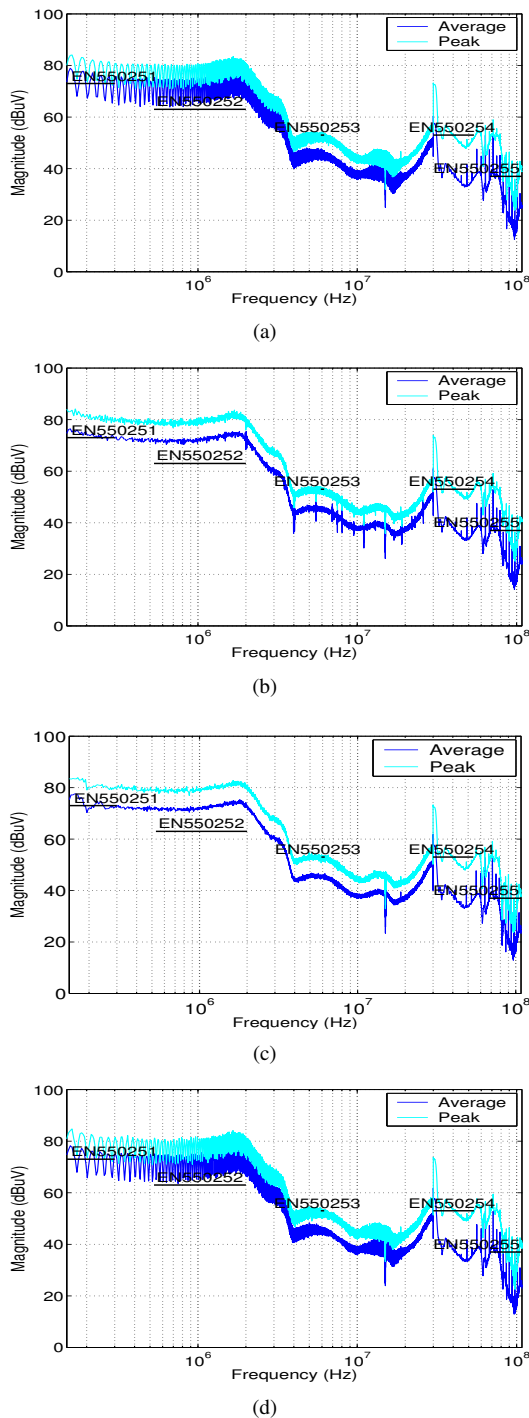


Fig. 13. Conductive EMI of the randomized SMPC ($\mathcal{R} = \pm 20\%$, $D = 70\%$): (a) RPPM, (b) RPWM, (c) RCFMFD, and (d) RCFMVD

ductive noise ripple within low-frequency range of up to 2 MHz, and ensured an adequate difference between the peak- and average-values of the conductive noise through-

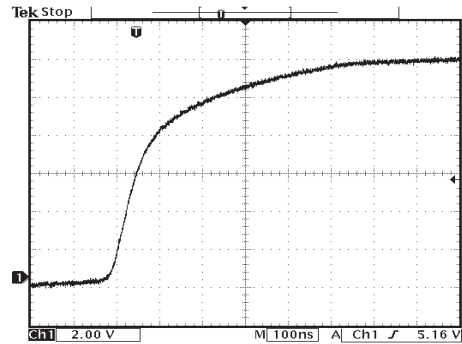


Fig. 14. Improved output voltage of the main switch at the turn-off

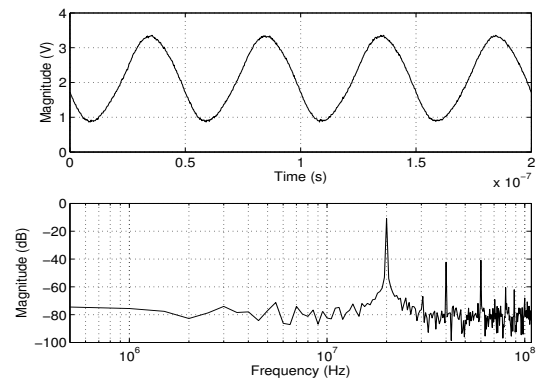


Fig. 15. DFT of the quartz clock signal

out the whole frequency range.

5 CONCLUSION

This paper has outlined a comparative investigation into the effects of different random modulation schemes on the PSD and conductive EMI in SMPC, compared to the ordinary PWM. By two typical examples of SMPC it has been clearly demonstrated that all the considered randomization schemes can gradually spread discrete frequency harmonic power over the whole frequency spectrum. In the first case, randomization improved the performance of the boost rectifier throughout almost the whole frequency range, except at lower frequencies where a small increment of the THD was detected but the PF was still close to unity. In the second case, optimization measures within the DC-DC buck converter structure could fully eliminate the use of an EMI input filter, regardless of the used modulation (PWM or RPWM).

REFERENCES

- [1] C. R. Paul, *Introduction to Electromagnetic Compatibility*. New York, USA: John Wiley & Sons Inc., 2006.

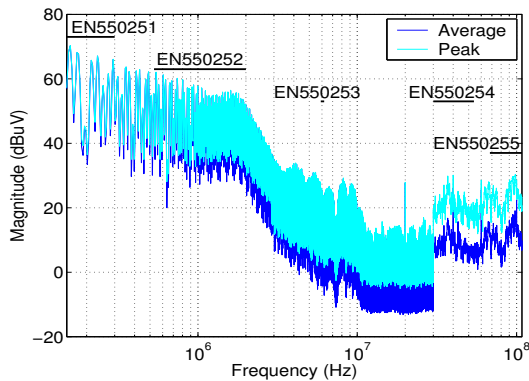


Fig. 16. EMI measurements of redesigned SMPC

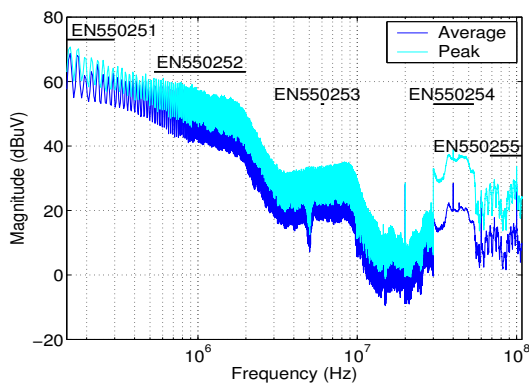


Fig. 17. Conductive EMI of the half-bridge SMPC topology with RPWM ($\mathfrak{R} = \pm 20\%$, $D = 70\%$)

- [2] R. Redl, "Power electronics and electromagnetic compatibility," in *27th Power Electronics Specialists Conference Record*, vol. 1, (Baveno, Italy), pp. 15–21, June 1996.
- [3] F. Mihalič and M. Milanovič, "Wide-band analysis of the random modulated boost rectifier," in *Proceedings of the 31st Power Electronics Specialists Conference*, (Galway, Ireland), pp. 946–951, June 2000.
- [4] EN 55022, *Limits and methods of measurement of radio disturbance characteristics of information technology equipment*, 1994.
- [5] EN 55025, *Radio disturbance characteristics for protection of receivers used on board vehicles, boats, and on devices – Limits and methods of measurements*, 2004.
- [6] EN 61000-3-2, *Electromagnetic compatibility (EMC) - Part 3: Limits - Section 2: Limits for harmonic current emission (equipment input current ≤ 16 A per phase)*, 1995.
- [7] K. K. Tse, H. S. Chung, S. Y. R. Hui, and H. C. So, "A comparative investigation on the use of random modulation schemes for DC/DC converters," *IEEE Trans. on Industrial Electronics*, vol. 47, no. 2, pp. 253–263, 2000.
- [8] R. Giral, A. E. Aroudi, L. Martínez-Salamero, R. Leyva, and J. Maixe, "Current control technique for improving EMC in power converters," *Electronics Letters*, vol. 37, no. 5, pp. 274–275, 2001.
- [9] P. W. Clarke, "Self-commutated thyristor DC-to-DC converter," *IEEE Trans. on Magnetics*, vol. MAG-6, no. 1, pp. 10–15, 1970.
- [10] V. K. Madiseti and D. B. Williams, *The Digital Signal Processing Handbook*. Boca Raton, FL: CRC Press, 1998.
- [11] The Math Works Inc., Natick, Massachusetts, *Matlab: Signal Processing Toolbox User's Guide*, 2006.
- [12] A. M. Stanković and H. Lev-Ari, "Randomized modulation in power electronic converter," *Proceedings of the IEEE*, vol. 90, no. 5, pp. 782–799, 2002.
- [13] S. L. Marple, *Digital Spectral Analysis with Applications*. Englewood Cliffs, NJ: Prentice Hall, 1987.
- [14] R. L. Kirlin, M. M. Bech, and A. M. Trzynadlowski, "Analysis of power spectral density in PWM inverters with randomized switching frequency," *IEEE Trans. on Industrial Electronics*, vol. 49, no. 4, pp. 486–499, 2002.
- [15] J. G. Proakis and D. G. Manolakis, *Digital Signal Processing: Principles, Algorithms and Applications*. New York: Macmillan, 2nd ed., 1992.
- [16] N. O. Sokal, K. K. Sum, and D. C. Hamill, "A capacitor-fed, voltage-step-down, single phase, non-isolated rectifier," in *Proceedings of the 13th Applied Power Electronics Conference*, (Anahaim, CA), pp. 208–215, February 1998.
- [17] O. García, J. A. Cobos, R. Prieto, P. Alou, and J. Uceda, "Single phase power factor correction: a survey," *IEEE Trans. on Power Electronics*, vol. 18, no. 3, pp. 749–755, 2003.
- [18] B. Terzić, G. Majić, and A. Slutej, "Stability analysis of three-phase PWM converter with LCL filter by means of nonlinear model," *Automatika*, vol. 51, no. 3, pp. 221–232, 2010.
- [19] K.-S. Kim, Y.-G. Jung, and Y.-C. Lim, "A new hybrid random PWM scheme," *IEEE Trans. on Power Electronics*, vol. 24, no. 1, pp. 192–200, 2009.
- [20] T. Tanaka and T. Ninomiya, "Random-switching control for DC-to-DC converter: analysis of noise spectrum," in *23rd PESC'92 Record*, vol. 1, (Toledo, Spain), pp. 579–586, June 1992.
- [21] T. G. Habetler and D. M. Divan, "Acoustic noise reduction in sinusoidal PWM drives using a randomly modulated carrier," *IEEE Trans. Power Electronics*, vol. 6, pp. 356–363, July 1991.



F. Mihalič received the B.S., M.S. and Ph.D. degrees in electrical engineering from the Faculty of Electrical Engineering and Computer Science, University of Maribor, Slovenia in 1988, 1995 and 2000, respectively. After graduating he worked four months at the electronics factory Elrad in Gornja Radgona, Slovenia. From 1989 to 2002 he was a Teaching Assistant for the power electronics at the Faculty of Electrical Engineering and Computer Science, University of Maribor. In 2000, he spent 3 months at the University of Minho in Guimarães, Portugal as a visiting scholar within the EU Socrates-Erasmus program. From 2002 to 2007 he has been an Assistant Professor and since 2007 an Associate Professor at the University of Maribor. His research interests include DC-DC converters modeling, high power factor correction techniques, random modulation strategies, signal processing and reduction of electromagnetic interference. He is an IEEE Member in Industrial Electronics-, Power Electronics- and Electromagnetic Compatibility Society, where he also serves as a reviewer.

AUTHORS' ADDRESSES

Prof. Franc Mihalič, Ph.D.

University of Maribor,

Faculty of Electrical Engineering and Computer Science,

Institute of Robotics,

Smetanova 17, 2000, Maribor, Slovenia

email: fero@uni-mb.si

Received: 2012-01-13

Accepted: 2012-03-21